

# SIMPLIFIED SPHERICAL NEAR-FIELD ACCURACY ASSESSMENT

Greg Hindman & Allen C. Newell  
Nearfield Systems Inc.  
19730 Magellan Drive  
Torrance, CA 90502

## ABSTRACT

Spherical near-field measurements have become a common way to assess performance of a wide variety of antennas. Published reports on range error assessments for spherical near-field ranges however are not very common. This is likely due to the perceived additional complexity of the spherical near-field measurement process as compared to planar or cylindrical measurement techniques. This paper will establish and demonstrate a simple procedure for characterizing the performance of a spherical near-field range. The measurement steps and reporting can be largely automated with careful attention to the test process. We will summarize the process and document the accuracy of a spherical near-field test range at NSI using the same NIST 18 terms commonly used for planar near-field measurements.

**Keywords:** NIST, 18-term, error evaluation, absorber, reflection, spherical near-field, suppression, MARS

## 1. Introduction

This paper describes a simplified process for establishing the performance of a typical spherical near-field measurement system. For planar near-field measurements, the ‘NIST’ 18-term budget, first described in [1], has been fairly well accepted in industry, but there have been relatively few documented results of its application to spherical near-field measurements. Hansen [2] includes a chapter on error analysis, but it is somewhat difficult to translate into practical tests. In [3], Hess identifies quite a number of additional alignment related errors, and expands the list to a total of 50 terms. Having to deal with 50 terms, or even 18 terms can be intimidating. Here we will not attempt to address all possible error sources, but focus on a number of the largest contributors in the 18 term list and identify how to make a reasonable engineering assessment of the important system errors. The antenna we will use in the tests is the NSI-RF-SG284 S-band Standard Gain Horn. A sample 3-D radiation patterns of the horn is shown in Figure 1. The E-plane pattern cuts over the full 2.6 to 3.95 GHz band are shown in Figure 2. We tested the SGH on NSI’s 700S-60 spherical near-field scanner shown in Figure 3.

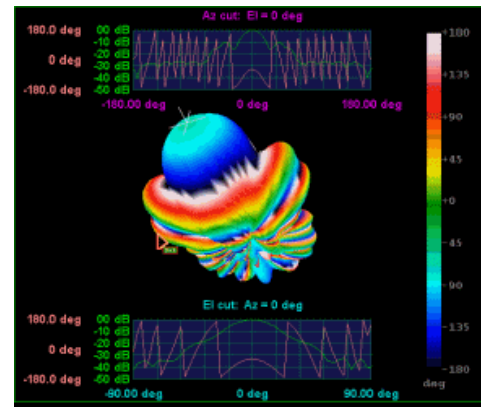


Figure 1 – Typical radiation pattern of NSI-RF-SG284 Standard Gain Horn used in the testing

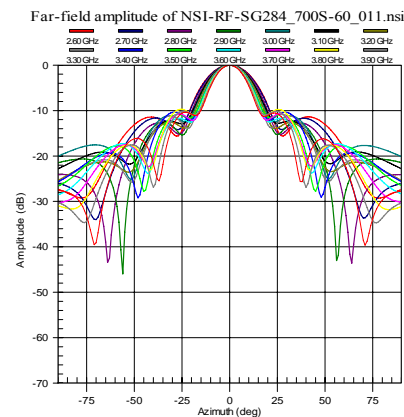


Figure 2.– E-plane pattern cuts at each frequency on NSI-RF-SG284 Standard Gain Horn used.



Figure 3 – NSI-700S-60 SNF scanner used in the testing

## 2. How to keep it simple

One key factor in keeping the accuracy assessment simple is to establish the appropriate tradeoffs between test accuracy and test time. One can usually improve on the position accuracy term by running tests more slowly, or taking fewer frequencies, but you would then be suffering the additional test time, or reduction in data completeness. The trick is to establish reasonable accuracy guidelines to allow your testing to be as efficient as possible. Determining the right choice of parameters to vary, and analyzing and interpreting the results can be difficult.

NSI uses the self-comparison technique often to evaluate the effects of error sources on the measurement results. It is useful to establish a ‘truth model’, or our best estimate of the ‘correct’ measurement result, and use this for comparison to results derived with compromises in accuracy in favor of reduced test time. For this, we use three steps: 1 - take the data with minimal or controlled position errors (stop motion or slow scanning); 2 - average out range reflection and alignment errors with a redundant scanning technique to be described; 3 - apply NSI’s Mathematical Absorber Reflection Suppression (MARS) technique [4]. These three steps will help to derive the ‘true’ antenna radiation pattern for use in subsequent self-comparison measurements to derive the effect of a number of the error sources.

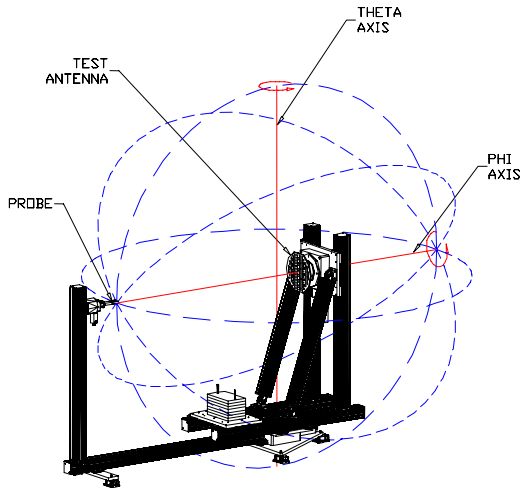


Figure 4 – Coordinate system for typical spherical near-field rotator system

NSI’s spherical systems can acquire a double data set on the AUT; basically two redundant spheres of data acquired with different rotation segments of the rotators (see Figures 4 & 5). The ‘360phi’ data set is taken with full 360° phi rotation of the AUT, but with only 0-180° motion in theta. In this mode, the AUT’s Z axis will only be looking at one side of the chamber during the

measurement. The ‘180phi’ data set is taken with only 180° phi rotation, but a full 360° rotation in theta. In this mode, the AUT’s Z axis looks at all four of the side walls in the chamber. This double data set can also help reduce effects of the residual alignment errors in the system. This technique is further described in a paper by the authors [5].

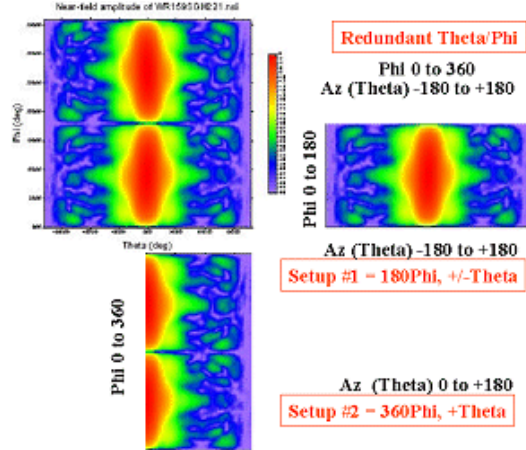


Figure 5 – Redundant data set through full rotation of theta and phi rotators, versus the two full spheres that can be derived for the 180 phi or 360 phi configurations

## 3. Spherical alignment

The alignment of the rotation axes of the rotators in a spherical system is critical. NSI has developed an electrical alignment technique which helps to check and optimize the alignment of the system using actual measured RF data, without the need to remove the probe and AUT [6]. The basic concept involves comparing a theta pattern cut with AUT phi at 0° versus one taken with phi at 180°. These should be identical, but will vary due to misalignments. The amplitude error is primarily caused by theta axis pointing error, and the phase error is primarily caused by intersection error between the theta and phi axes, allowing us to largely separate and optimize the two errors. The results of the NSI software’s analysis of the alignment data is shown in Figure 6.

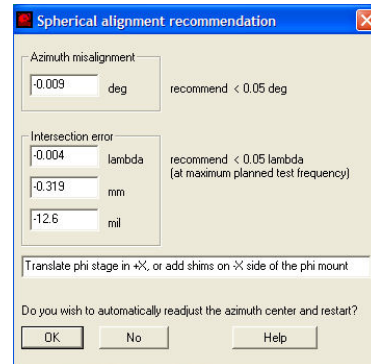


Figure 6 – Result of NSI self-alignment check, showing derivation of theta and phi alignment information

One additional advantage of NSI's option of measuring full redundant data with both 180 phi and 360 phi data sets is that in averaging the two data sets, it also helps to reduce the effects of the residual misalignment of the system, since each of the test geometries has a different sensitivity to the alignment errors [7] [8].

#### 4. Review of the 18 terms for side lobe accuracy

In this paper, we will limit ourselves primarily to errors relating to side lobe accuracy. Similar techniques can be applied to derive the appropriate effects on gain accuracy and cross-polarization accuracy. Table 1 shows a summary of the techniques used.

**Term 1 - Probe relative pattern.** For spherical near-field measurements, the probe pattern correction is less important than in planar measurements since only the probe pattern over the subtended angular region illumination the AUT is of significance. To estimate the error, we can perturb the processed SNF result by applying an error in the probe correction model used and determine the effect on the far-field result. An easy way to do this in the NSI software is to use the probe pattern model from the next lower frequency probe band, as this will be a gross error and will bound an estimate on the uncertainty. Figure 7 shows the error level is -54 dB at 2.6 GHz which corresponds to a 0.16 dB error in a -20 dB side lobe level. The results for all frequencies are shown on row 1 on the 18-term uncertainty summary in table 2.

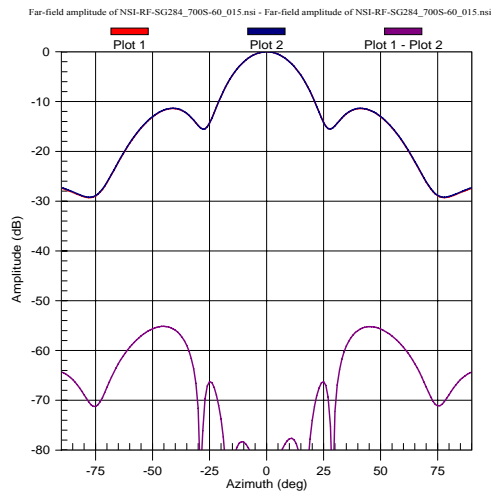


Figure 7 – Error induced on E-plane pattern by applying a worst case probe pattern error

**Term 2 - Probe polarization.** This term will be negligible for side lobe analysis at the level of interest.

**Term 3 - Probe gain.** This term is not applicable to side lobe analysis

**Term 4 - Probe alignment.** For broadbeam probes like the Open Ended Waveguide (OEWG) probe used here, the effects of probe alignment will be negligible and are considered covered in the estimate of term 1 above.

**Terms 5 and 6 - Normalization constant and Impedance mismatch.** These are related to gain measurements and are not applicable to side lobe analysis

**Term 7 - AUT alignment error.** This can be determined by evaluation of the mechanical alignment of the antenna versus the range reference. If, however, one is using the test results for comparisons, which are referenced to the electrical beam peak of the antenna pattern, this term can usually be ignored.

**Term 8 - Data point spacing.** We use a simple process of self-comparison using a data set at the normal Nyquist sample spacing versus another one that is taken at half the angular spacing. See table 2 for results.

**Term 9 - Truncation.** This can easily be evaluated by truncating a full measurement data set in theta down to a smaller angular range, and evaluating the result. Here, we are taking a full 360° data set in theta, so there is no truncation effect, other than the unavoidable blockage of the back lobe of the antenna by the phi rotator and mount. This will not affect the front hemisphere data for most medium to high gain antennas. For lower gain antennas, it is usually possible to position the antenna so that a null or low energy region of its radiation pattern is directed toward the mounting structure.

**Term 10 and 11 - XY and Z errors.** In a planar NF range, these are typically evaluated using analysis of the scanner probe position errors. In a spherical NF range, the spherical measurement surface will be imperfect due to inaccuracies of the positioners and misalignments of these positioners. Mechanical measurements can be made and analyzed for this term; however, we can also derive an estimate from an analysis and self-comparison of a redundant SNF measurement result. As described above, the NSI system can acquire a redundant data set and allow processing of the 180phi versus the 360phi data sets. Each data set has a different sensitivity to the rotator alignment errors as shown in [8]. For our test system, we also did a brief sensitivity study and derived the result in Figure 8, which shows that the 360phi data set has a much greater side lobe error sensitivity to theta-zero misalignments than the 180phi data set. The 180phi data set is about half as sensitive to the alignment errors, but you can also see that the combined result of the redundant data yields a much lower error – about ¼ the sensitivity of the 360phi data set.

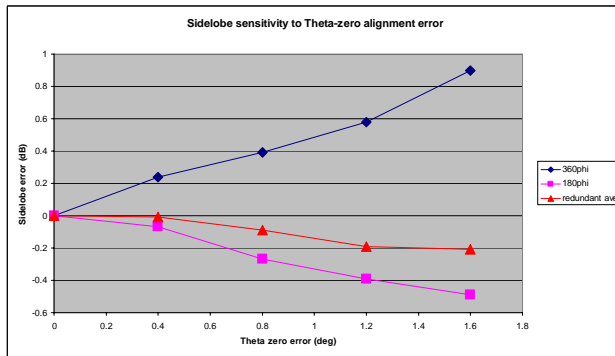


**Figure 8 – Alignment sensitivity curve, showing side lobe error due to theta-zero misalignment for different test geometries**

For the side lobe error evaluation, we will use a comparison of the 180phi result to the combined result of the redundant set as an estimate of the effect of the XYZ position errors in the system. Since we are taking data on-the-fly, we are also inducing some position error in the measurements which is speed dependent, so we compare our redundant data set, taken at very slow speed (3°/sec), to the non-redundant data set taken at the normal fast scan speed (30°/sec). The two spherical data sets will also be sensitive to reflections in different parts of the range, so to isolate the effect of alignment, we apply the NSI MARS reflection suppression algorithm on each data set before the comparison. See results in table 2.

**Term 12 - Probe/AUT mutual coupling.** For this error, as in planar, we vary the AUT to probe spacing. Here we have simply acquired another data set with probe moved back  $\frac{1}{4} \lambda$ , which increases the measurement radius by that amount. Note that this movement of the probe also will change the character of the room reflections, so some of the term 16 room reflection effect will invariably be included in this result for term 12. See results in table 2.

**Term 13 - Receiver amplitude linearity.** This term is typically evaluated using a perturbation of an existing data set with non-linearity profile from the receiver vendor. Here we are using an Agilent PNA and have used Agilent spec data for the evaluation, which results in a side lobe error estimate of 0.12 dB.

**Term 14 - System phase error.** In planar NF, this term is usually dominated by the effects of flexible cables in the X and Y motion. In our spherical NF system, we are using rotary joints for each of the 3 rotators, and their effects on the results will be much less than in a case where flexible cables were used. To derive an estimate of this error source, we can use specifications or measured data on the rotary joints to perturb an existing data set, or we can do an on-system self-comparison test. For a well aligned system, we can do a simple rotation test of the AUT phi and probe polarization axes, keeping them co-

polarized over 360° rotation, as an upper bound on the rotary joint amp and phase variation. On our range, this results in a 0.08 dB p-p amp error and 1° phase error, and superimposing that error on a measured data set gives the results shown in Figure 9. A -54 dB error level gives about a 0.18 dB effect on the -20 dB side lobe.

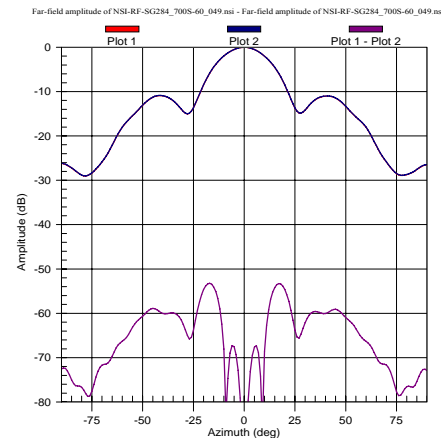


**Figure 9 – Effect of systematic phase measurement of rotary joint error on E-plane cut**

**Term 15 - Receiver dynamic range.** A common method is to insert an attenuator in the path, reducing the power level into the receiver, and re-measuring the results for comparison. This involves an additional measurement, and suffers from repeatability error as well as the dynamic range effects. An alternate and simpler approach, used here, is to simply observe the SNR of the near-field signal on-axis and use this for the dynamic range term. In our case, the on-axis SNR is about 65 dB, giving only a 0.05 dB affect on a -20 dB side lobe.

**Term 16 - Room scattering.** It is common to derive this from a measurement with the AUT shifted to a different position, however this involves removal and reinstallation of the antenna and is often difficult to perform without introducing undesirable alignment errors which can corrupt the ability to determine just the room scattering effect. An alternate simpler approach is used here, taking advantage of the redundant sphere data. Since the 180phi and 360phi data sets will have different reflection errors in the chamber, we simply compare the 180phi data set to the redundant processed data set to derive the chamber error term. Note that we can just process the data from the previously measured slow scan taken for term 10, so no new measurement is required. Results are in table 2.

**Term 17 - Leakage.** Leakage is evaluated by terminating the probe cable and measuring and transforming a full 2D leakage data set to determine its effect on the far-field result. As seen in table 2, the results are fairly small.

**Term 18 - Random amplitude & phase errors.** This term is basically the system repeatability, and is simply evaluated by comparison of two data sets taken back to back with no changes. This term will be sensitive to the receiver averaging or bandwidth / integration time, so the receiver needs to be set up appropriately and these settings maintained for subsequent tests, or else the random term will need to be re-evaluated. Note that a portion of this term is actually included in most of the other terms which involve measurement comparison, so if the repeatability effect is not significantly better than the terms being evaluated, the combined rss result will be somewhat too pessimistic (conservative).

**Table 1 - Summary of the 18 term self-comparison techniques used in this process**

NIST Term	Description	Self-comparison Technique
1	Probe pattern	Reprocess with probe pattern perturbed using an adjacent freq. band
2	Probe pol.	n/a for side lobes
3	Probe gain	n/a for side lobes
4	Probe align	Negligible for OEWG
5	Norm constant	n/a for side lobes
6	Imp. mismatch	n/a for side lobes
7	AUT Alignment	n/a unless need mechanical ref
8	Data spacing	Test normal vs. double density
9	Truncation	Truncate existing data set
10,11	XYZ errors	Compare fast speed, 180 phi only, to slow scan with redundant data
12	Probe-AUT reflections	Test with changed probe radius $\frac{1}{4}\lambda$
13	Linearity	Perturb data with vendor spec data
14	Systematic phase	Coupling test between rotary joints
15	Dynamic range	Evaluation of system SNR
16	Room Scattering	Compare 180phi versus redundant data set from same scan
17	Leakage	Test with cable loaded
18	Random Errors	Repeatability

### 5. Overall 18-Term Uncertainty Results

The summary of the 18 term analysis is shown in table 2 for the spherical near-field range with MARS reflection suppression software enabled for the low, middle, and high frequency range of the WR-284 SGH and probe. We have also listed the performance at the low frequency only without the MARS reflection suppression technique. The results shown can be achieved with only a moderate

amount of testing and analysis over only a 1-2 day period, and will give a good estimate of the system performance. Additional work can certainly be done to reduce some of the terms by adjusting test parameters and performing appropriate tradeoffs. For instance, sacrificing test time by slower scanning speed, or reducing number of frequencies, or performing full redundant data sets for all further data evaluation, can help reduce the listed error sources. One can see that the MARS reflection suppression can provide a significant improvement in the chamber performance terms – probe to AUT reflections (12), and room scattering (16), however it also improves our ability to isolate out other terms which would be otherwise swamped by the poor absorber performance.

### 6. Summary

This paper has identified a number of fairly straightforward tests to help the engineer more readily document the accuracy of a typical spherical near-field range. A number of unique self-comparison tests we have identified can reduce the effort required to get to an acceptable error budget. NSI's MARS reflection suppression technique can improve the reflection levels in a traditional anechoic chamber, allowing improved accuracy as well as the ability to use existing chambers down to lower frequencies than the absorber size might indicate.

### 7. REFERENCES

- [1] Newell, A.C. Error analysis techniques for planar near-field measurements, IEEE Trans. Antennas & Propagation, AP-36, p. 581 1988.
- [2] Hansen, J. E., Editor (1988) "Spherical Near-Field Antenna Measurements", London: Peregrines.
- [3] Hess, D. W. "An Expanded Approach to Spherical Near-Field Uncertainty Analysis", AMTA 24<sup>th</sup> Annual Meeting & Symposium, Cleveland, OH, Oct. 2002.
- [4] Hindman, G, Newell, A.C., " Reflection Suppression To Improve Anechoic Chamber Performance", AMTA Europe 2006, Munch, Germany, Mar. 2006.
- [5] Hindman, G, Newell, A.C., " Spherical Near-Field Self-Comparison Measurements", AMTA 26th Annual Meeting & Symposium, Atlanta, GA, Oct. 2004.
- [6] Newell, A. C., Hindman, G., "The alignment of a spherical near-field rotator using electrical measurements" AMTA 19th annual Meeting and Symposium, Boston, MA, 1997.
- [7] Newell, A. C., Hindman, G., "Quantifying the effect of position errors in spherical near-field measurements", AMTA 20<sup>th</sup> annual Meeting and Symposium, Montreal, Canada, 1998.
- [8] Newell, A.C., "The effect of measurement geometry on alignment errors in spherical near-field

measurements". AMTA 21st Annual Meeting &  
Symposium, Monterey, California, Oct. 1999.

**Table 2 - 18-Term Uncertainty Summary**

The summary of the 18 term analysis is shown below for the spherical near-field range with MARS reflection suppression software enabled for the low, middle, and high frequency range of the WR-284 SGH and probe. At the low frequency, we have also shown the expected error without the MARS reflection suppression.

	Frequency (GHz)	Error on -20dB side lobe (dB)			
		2.6	2.6	3.3	4.0
NIST Term	Description				
1	Probe pattern	0.14	0.16	0.20	0.12
2	Probe polarization	n/a	n/a	n/a	n/a
3	Probe gain	n/a	n/a	n/a	n/a
4	Probe alignment	0	0	0	0
5	Normalization constant	n/a	n/a	n/a	n/a
6	Impedance mismatch	n/a	n/a	n/a	n/a
7	AUT Alignment Error	n/a	n/a	n/a	n/a
8	Data spacing	0.28	0.22	0.34	0.31
9	Truncation	n/a	n/a	n/a	n/a
10,11	XYZ errors	1.32	0.66	0.66	0.92
12	Probe-AUT reflections	3.30	1.03	0.45	0.50
13	Linearity	0.12	0.12	0.12	0.12
14	Systematic phase	0.18	0.18	0.18	0.18
15	Dynamic range	0.05	0.05	0.05	0.05
16	Room Scattering	0.50	0.22	0.28	0.12
17	Leakage	0.01	0.01	0.02	0.04
18	Random Errors	0.06	0.06	0.04	0.04
	<b>RSS (dB)</b>	<b>3.61</b>	<b>1.29</b>	<b>0.96</b>	<b>1.13</b>
	<b>Processing:</b>	<b>None</b>	<b>MARS</b>	<b>MARS</b>	<b>MARS</b>